JOURNAL OF BACTERIOLOGY, Oct. 2007, p. 6773–6786 Vol. 189, No. 19
0021-9193/07/$08.00+0 doi:10.1128/JB.00827-07

Salicylic Acid, Yersiniabactin, and Pyoverdin Production by the Model Phytopathogen *Pseudomonas syringae* pv. tomato DC3000: Synthesis, Regulation, and Impact on Tomato and *Arabidopsis* Host Plants[▽]†

Alexander M. Jones, Steven E. Lindow, and Mary C. Wildermuth*

Department of Plant and Microbial Biology, 111 Koshland Hall, University of California at Berkeley, Berkeley, California 94720-3102

Received 28 May 2007/Accepted 16 July 2007

A genetically tractable model plant pathosystem, *Pseudomonas syringae* pv. tomato DC3000 on tomato and *Arabidopsis thaliana* hosts, was used to investigate the role of salicylic acid (SA) and iron acquisition via siderophores in bacterial virulence. Pathogen-induced SA accumulation mediates defense in these plants, and DC3000 contains the genes required for the synthesis of SA, the SA-incorporated siderophore yersiniabactin (Ybt), and the fluorescent siderophore pyoverdin (Pvd). We found that DC3000 synthesizes SA, Ybt, and Pvd under iron-limiting conditions in culture. Synthesis of SA and Ybt by DC3000 requires *pchA*, an isochorismate synthase gene in the Ybt genomic cluster, and exogenous SA can restore Ybt production by the *pchA* mutant. Ybt was also produced by DC3000 in planta, suggesting that Ybt plays a role in DC3000 pathogenesis. However, the *pchA* mutant did not exhibit any growth defect or altered virulence in plants. This lack of phenotype was not attributable to plant-produced SA restoring Ybt production, as the *pchA* mutant grew similarly to DC3000 in an *Arabidopsis* SA biosynthetic mutant, and in planta Ybt was not detected in *pchA*-infected wild-type plants. In culture, no growth defect was observed for the *pchA* mutant versus DC3000 for any condition tested. Instead, enhanced growth of the *pchA* mutant was observed under stringent iron limitation and additional stresses. This suggests that SA and Ybt production by DC3000 is costly and that Pvd is sufficient for iron acquisition. Further exploration of the comparative synthesis and utility of Ybt versus Pvd production by DC3000 found siderophore-dependent amplification of *ybt* gene expression to be absent, suggesting that Ybt may play a yet unknown role in DC3000 pathogenesis.

Iron is essential for most forms of life and is a critical factor in pathogenesis (62). Pathogenic bacteria, which rely on the host for iron nutrition, must be able to efficiently compete for iron. Most bacteria require 10^{-6} to 10^{-7} M levels of bioavailable iron for optimal growth (39). In mammalian biological fluids, available iron is estimated to be less than 10^{-18} M (38, 78), as hosts limit free iron to prevent oxidative damage and its availability to pathogenic organisms. One common mechanism by which bacterial pathogens acquire iron is through the use of siderophores. Siderophores are low-molecular-weight peptidic molecules with high specificity and affinity for ferric iron (K_a, 10^{22} to 10^{50}). Under iron-limiting conditions, siderophores are produced via nonribosomal peptide synthesis, excreted by the cell, and then imported via specific receptor/transporters once bound to Fe^{3+} (21). In this way, cells are able to scavenge iron from iron-depleted environments.

Regulation of siderophore biosynthesis appears to be highly fine-tuned, with multiple layers of control, including repression by Fe^{2+}-Fur under iron-rich conditions, siderophore-dependent amplification via TonB-dependent siderophore receptor/transporters (such as FpvA) or AraC transcriptional regulators (such as PchR), and posttranscriptional regulation by antisense RNAs (8, 66, 76). Emerging evidence also indicates a link between quorum sensing (cell density-dependent regulation) and siderophore biosynthesis. For example, quorum-sensing *Pseudomonas aeruginosa* mutants exhibit reduced pyoverdin (Pvd) production (69). Furthermore, dual regulation of siderophore biosynthesis by iron and oxidative stress has been observed in certain cases (e.g., catecholate siderophore biosynthesis by *Azotobacter vinelandii* [71]), consistent with the capacity of intracellular siderophores to function as cytoprotective antioxidants by limiting the generation of highly reactive hydroxyl radicals produced via the Fenton reaction.

In terms of pathogenesis, the importance of siderophores in bacterial virulence on mammalian hosts has been well demonstrated. For example, yersiniabactin (Ybt) is required for full virulence of *Yersinia pestis* and *Klebsiella pneumoniae* infections of mice (6, 46), and Pvd is needed for virulence of *P. aeruginosa* in burned mice (51). Siderophore synthesis and utilization is under constant selective pressure as hosts evolve means to counteract pathogenic iron acquisition by siderophores and bacteria develop counterevasive strategies (33). For example, the mammalian protein siderocalin binds catecholic siderophores such as enterobactin and bacillibactin, making them ineffective in bacterial iron acquisition.

A number of bacteria synthesize multiple high-affinity siderophores of different structural classes, allowing them to bypass host-evolved defenses and/or serve distinct functional roles. For example, *Bacillus anthracis* synthesizes both the 2,3-catecholate siderophore bacillibactin and the unusual citrate–3,4-catecholate siderophore petrobactin, whose unique struc-

* Corresponding author. Mailing address: Department of Plant and Microbial Biology, 111 Koshland Hall, University of California, Berkeley, CA 94720-3102. Phone: (510) 643-4861. Fax: (510) 642-4995. E-mail: Wildermuth@nature.berkeley.edu.

† Supplemental material for this article may be found at http://jb.asm.org/.

▽ Published ahead of print on 27 July 2007.

ture is not recognized by siderocalin (1). As expected, *B. anthracis* mutants in bacillibactin synthesis exhibit no defect in mouse virulence, whereas petrobactin mutants exhibit reduced virulence (17). In the case of *A. vinelandii*, in contrast to synthesis of the Pvd-like siderophore azotobactin, catecholate siderophore synthesis is under dual regulation by iron and oxidative stress, consistent with its cytoprotective antioxidant role (71). Another example is the probiotic *Escherichia coli* strain Nissle 1917, which produces four siderophores: the catecholates enterobactin and salmochelin, the hydroxamate aerobactin, and the mixed-type siderophore Ybt. These siderophores exhibit maximal production at different pHs, in agreement with their relative affinities for iron(III) at these pHs (72). Furthermore, an *E. coli* N1917 Ybt$^-$ mutant exhibited reduced growth in competition with the wild-type strain at neutral but not acidic pHs, consistent with increased Ybt production and higher affinity for iron at neutral pHs (72).

In contrast to mammalian pathosystems, siderophore production by phytopathogens and their role in virulence on plant hosts has not received much attention. A clear role for siderophores in plant-pathogen interactions was first established for the pectinolytic enterobacterium *Dickeya dadantii*, formerly known as *Erwinia chrysanthemi*, the causative agent of soft rot on a great variety of plants (29, 30), and has been recently observed for several fungal phytopathogens (28, 57). *D. dadantii* 3937 infection requires two structural classes of high-affinity siderophores, chrysobactin and achromobactin, with mutants in either high-affinity iron transport system compromised in their virulence on the African violet (*Saintpaulia ionantha*) (34). In contrast, single-siderophore biosynthetic mutants in other bacterial phytopathogens have not exhibited virulence defects under the conditions tested. For example, *Pseudomonas syringae* pv. syringae B301D, a pathogen of stone fruit trees such as wet cherry (*Prunus avium* L.), does not require Pvd for virulence on immature sweet cherry fruits (19). Similarly, virulence of *Agrobacterium tumefaciens* B6 and C58 strains, which cause crown gall disease, was not significantly compromised by the inability to produce either agrobactin (47) or an uncharacterized high-affinity siderophore (65). There are a number of possible reasons for the lack of virulence phenotype for these siderophore mutant strains, including the compensatory action of another high-affinity siderophore and/or the plant growth environment or particulars of the infection assay.

In order to fully explore the likely complex role of siderophores and iron in phytopathogenesis, we employ the use of a widely studied pathosystem with extensive genomic and genetic resources available for both the bacterium and plant hosts. *Pseudomonas syringae* pv. tomato DC3000, a model phytopathogen (11), causes bacterial speck of tomato (*Solanum lycopersicum*, formerly *Lycopersicon esculentum*) (22), a worldwide disease of economic significance, and is also highly virulent on the model plant *Arabidopsis thaliana* (44, 77). In particular, the use of the *P. syringae* pv. tomato DC3000-*Arabidopsis* pathosystem allows one to readily and directly explore and assess bacterial and plant components mediating the interaction, as both bacterial and plant mutant lines can be easily constructed or are available (see, e.g., reference 3).

The genome of *P. syringae* pv. tomato DC3000 contains genes required for the synthesis of the mixed-type siderophore Ybt, derived from salicylic acid (SA), and the fluorescent siderophore Pvd (11). Whereas the role of bacterial Ybt in mammalian pathogenesis has been extensively studied, this is the first investigation into the role of Ybt in plant pathogenesis. As SA accumulates in plants such as *Arabidopsis* in response to pathogens including *P. syringae* pv. tomato DC3000, and pathogen-induced SA accumulation is required for basal plant host defense responses including the expression of a myriad of defense-related genes (24), we also wanted to assess the possibility of cross-talk between bacterial and plant SA production and utilization pathways. Therefore, our initial focus was to determine whether *P. syringae* pv. tomato DC3000 produces SA and Ybt and the role these compounds may play in virulence on tomato and *Arabidopsis* plant hosts. We then extended our studies to examine Pvd production and the comparative synthesis, regulation, and functional roles of these compounds in *P. syringae* pv. tomato DC3000 pathogenesis.

MATERIALS AND METHODS

Bacterial strains and culture. *P. syringae* pv. tomato isolate DC3000 (22), a DC3000 *pchA* mutant (this study), and *P. aeruginosa* PAO1 were streaked from 15% glycerol stock cultures maintained at −80°C. Three-milliliter liquid cultures were started with 5×10^8 CFU/ml (optical density at 600 nm [OD_{600}], 0.275) from cells grown on King's B (KB) agar plates with appropriate antibiotics. All cultures were grown in MOPS1 medium, MOPS (morpholinepropanesulfonic acid) medium (55) with $FeSO_4$ excluded and 1% Bacto CAS amino acids added. Stringent iron-limited cultures were grown in unused culture tubes (Fisher) supplemented with 150 μM 2,2′-dipyridyl (Sigma) unless otherwise noted. High-iron cultures were supplemented with 50 μM $FeCl_3$. Low-iron cultures were grown as with stringent iron-limited cultures except with washed culture tubes, resulting in more available iron. Under these low-iron conditions, growth of wild-type and *pchA* mutant DC3000 was iron-limited and similar. Cultures were incubated at 20°C with shaking at 2,750 rpm for 1 day unless otherwise noted. Dithiothreitol (DTT) cultures were supplemented with 100 μM DTT. H_2O_2 cultures were supplemented with 5 mM H_2O_2. Cultures for pH experiments were modified by adding 100 mM morpholineethanesulfonic acid and then adding concentrated NaOH to a pH of 5.7, 6.5, or 7.2. Cell density (in CFU per milliliter) was calculated from OD_{600} measurements (UV1601 Spectrophotometer; Shimadzu) and a *P. syringae* standard curve of CFU per milliliter versus OD_{600}. Data are reported as means and standard deviations of three replicates. Complete experiments were performed at least twice, with similar results.

Construction of the *P. syringae* pv. tomato DC3000 *pchA* mutant. A 534-bp *pchA* fragment lacking 5′ and 3′ coding regions was amplified using Turbo *Pfu* DNA polymerase (Stratagene) and the primers 5′-CACCAGGCACAAGGGCAATACCG-3′ and 5′-GCGCTGCATGACCTGTTCC-3′. The product was ligated into the pENTR/D-TOPO vector (Invitrogen) and recombined into the pLVC-D destination vector (pLVC18 [DNA Plant Technologies, Oakland, CA] with a gateway cassette cloned into the EcoRI site) in a gateway LR reaction (Invitrogen). The resulting pLVC-D+*ics* vector was then mated into DC3000 from *E. coli* DH5α in a triparental mating. Mated cells were grown on KB agar with 10 μg/ml tetracycline, and single colonies were isolated. The correct insertion of the vector into the genome was confirmed by PCR using *pchA* primers outside of the cloned region (5′-AACCCGCTGCCATCATTCA-3′ and 5′-CCTTAACGGGGGTCAGCAGA-3′) and primers annealing to the *attB1* and *attB2* cassette regions of the pLVC-D vector (5′-AGTTTGTACAAAAAAGCAGGCT-3′ and 5′-CTTTGTACAAGAAAGCTGGGT-3′, respectively). In culture under our experimental conditions (without antibiotic selection), we have found reversion of the *pchA* mutation to be minimal, as we have never detected SA, Ybt, or the presence of the intact *pchA* gene in *pchA* mutant cultures. For the in planta bacterial growth assays, the opportunity for selection is very limited, as there is little net growth (few generations).

Siderophore quantification and purification. For initial confirmation of siderophore identity by liquid chromatography-mass spectrometry (LC-MS) analysis, high-pressure liquid chromatography (HPLC) fractions for putative peaks were dried and submitted to the Vincent Coates Foundation Mass Spectrometry Laboratory (Stanford University). Ybt-Fe^{3+} was extracted from the supernatant (after addition of 100 μM $FeCl_3$) of a low-iron *P. syringae* pv. tomato DC3000 stationary-phase culture with 1 volume of ethyl acetate. The sample was dried and resuspended in 10% acetonitrile and then analyzed by HPLC. An acetoni-

trile gradient of 10 to 20% was applied from 1 to 6 min, 20 to 50% from 6 to 10 min, 50 to 65% from 10 to 20 min, 65 to 100% from 20 to 25 min, and 100 to 10% from 25 to 35 min. A fraction was collected around a dominant A385 peak and submitted for LC-MS. For Pvd-Fe^{3+} analysis, 100 μM $FeCl_3$ was added to supernatant from a low-iron wild-type DC3000 stationary-phase culture, and the supernatant was then concentrated 10-fold by evaporation with heating and vacuum. The sample was then analyzed by HPLC method 1 (14). A fraction was collected around the dominant A400 peak and submitted for LC-MS. For all Ybt and Pvd experiments, a Prevail C_{18} 5u 150- by 4.6-mm (Alltech) column maintained at 27°C was used on a Shimadzu SCL-10AVP series HPLC system equipped with a Shimadzu SPD-10AVP photodiode array detector and a Shimadzu RF-10AXL fluorescence detector.

For subsequent siderophore quantifications, 1-ml aliquots of liquid cultures were collected and 1 mM $FeCl_3$ was added. The mixture was then centrifuged at a relative centrifugal force of 20,000 for 2 min at 4°C. For each run, 50 μl of supernatant was analyzed by HPLC. The buffer used was 17 mM formic acid (pH 3.35), and an acetonitrile gradient of 0 to 2% was applied from 5 to 7 min, 2 to 70% from 7 to 20 min, 70 to 80% from 20 to 22 min, and 80 to 0% from 22 to 27 min. The flow rate was 1 ml/min. Ybt was quantified by the absorbance at 385 nm, with a standard curve using a Ybt standard provided by Chaitan Khosla (Stanford University) (59) and the reported molar extinction coefficient (ε = 2,884 [26]). Pvd-Fe^{3+} was quantified by the absorbance at 400 nm and the reported molar extinction coefficient (ε = 20,000 [18]). The Ybt-Fe^{3+} peak was identified by its elution time (~17.8 min) and absorbance spectrum compared with the Ybt standard. Consistent with published work on the atypical Pvd_{pss} (18), multiple distinct peaks were detectable as Pvd by absorbance spectrum with elution times of ~10.3, 10.75, and 11.4 min. Data are reported as means and standard deviations of three replicates. The complete experiment was performed twice with similar results.

SA extraction and quantification. Liquid cultures of *P. syringae* pv. tomato DC3000 and PAO1 strains were grown to stationary phase in low- and high-iron cultures. HCl was added to 25-ml supernatant samples from these cultures to a pH of 2 to 2.3. Samples were then extracted with 1 volume of ethyl acetate and evaporated to dryness in the dark and under a vacuum. Samples were then resuspended in 20% methanol and analyzed by HPLC using a 5 μM 15-cm by 4.6-mm ID Supelcosil LC-ABZ+Plus column (Supelco) preceded by an LC-ABZ+Plus guard column maintained at 27°C. The buffer used was 15% acetonitrile in 25 mM KH_2PO_4 (pH 2.5), and an acetonitrile gradient was applied. The flow rate was 1 ml/min. The concentration of acetonitrile was increased linearly to 20% over 6 min, followed by isocratic flow at 20% for 10 min, followed by a linear increase from 20% to 55% over 17.5 min, a linear increase from 43% to 66% over 5 min, isocratic flow at 66% for 2.5 min, a linear decrease from 66% to 15% over 5 min, and isocratic flow at 15% for 5 min. SA was detected by fluorescence at 407 nm after excitation at 305 nm and quantified with the calibration curve $y = 4418.2x$, with y in fluorescence area units and x in nanograms of SA. The SA peak was determined by elution time (~21 min) as determined by analysis of positive controls containing SA. Experiments were repeated three times with similar results.

Detection of Ybt in planta. *Arabidopsis thaliana* ecotype Columbia-0 (Col-0) plants were grown for 5 weeks in a 12-h light/dark cycle with photosynthetically active radiation (PAR) of ~150 $\mu Em^{-2}\,s^{-1}$ and sprayed with a 10 mM $MgSO_4$–0.05% Silwet L77 solution containing 5×10^8 CFU/ml of *P. syringae* pv. tomato DC3000 or the DC3000 *pchA* mutant. Negative-control treatments were sterile. Mature leaves from 12 plants were harvested in liquid nitrogen after 5 days. Leaves were then ground in 10 ml of H_2O and extracted twice with 1 volume of ethyl acetate. The organic layer was dried and the samples resuspended in H_2O and filtered before HPLC purification of the Ybt-Fe^{3+}-containing fraction, as described above. Samples were submitted to the Vincent Coates Foundation Mass Spectrometry Laboratory (Stanford University) for LC-MS analysis and detection of Ybt-Fe^{3+}. The complete experiment was performed twice with similar results.

MS. Samples for LC-MS analysis were resuspended in water and analyzed with a Thermo Fischer Alliance HPLC with a Luna C_{18} 2.1- by 150-mm column and a Thermo Fisher LCQ Classic Mass Spectrometer at the Vincent Coates Foundation Mass Spectrometry Laboratory (Stanford University). Confirmation of Ybt-Fe^{3+} and Pvd employed the separation gradients used to isolate the compounds (above) with electrospray ionization (ESI) positive-ion MS analysis. MS-MS fragmentation was performed on selected dominant ion peaks for further confirmation of compound identity.

For the in planta Ybt assays, the buffer used was 10% acetonitrile, and a gradient to 100% acetonitrile was applied. Isocratic flow at 10% for 1 min was followed by a linear increase to 20% over 5 min and then a linear increase to 50% over 4 min, a linear increase to 65% over 10 min, a linear increase to 100% over 5 min, isocratic flow at 100% for 3 min, a linear decrease to 10% over 5 min, and isocratic flow at 10% for 2 min. ESI positive-ion spectra from 50 to 1,500 *m/z* were collected for Ybt-containing fractions. Samples from plants infiltrated with *pchA* mutant DC3000 and $MgSO_4$ had no detectable Ybt-Fe^{3+}. ESI-positive spectra are shown for the same fraction as the sample from wild-type DC3000-infiltrated plants. MS-MS fragmentation was performed on selected dominant ion peaks to further verify Ybt-Fe^{3+}.

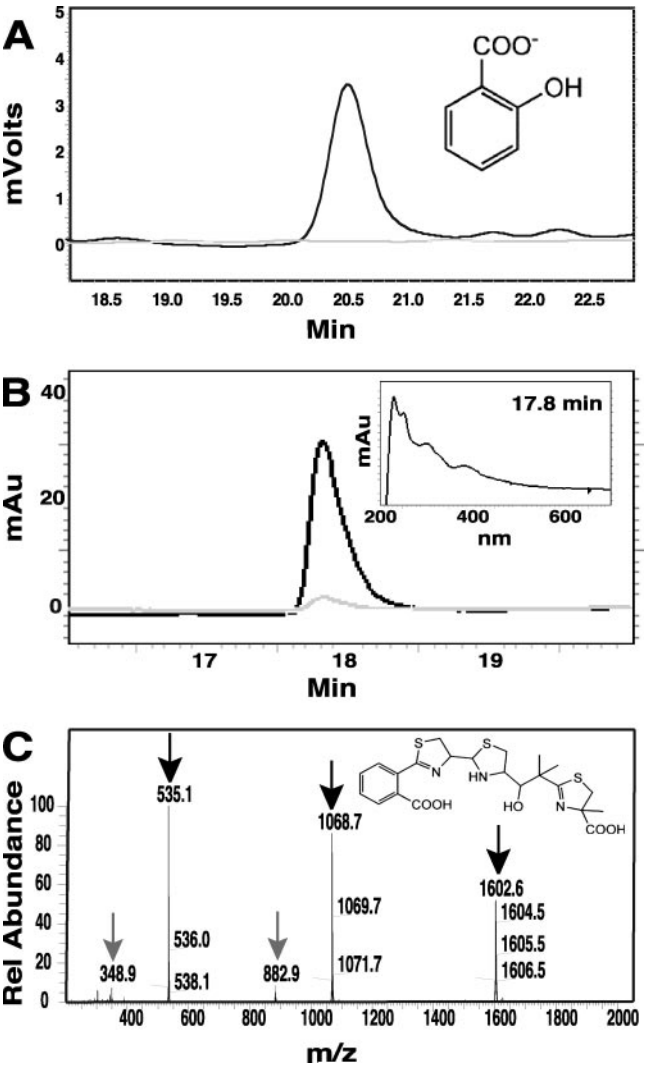

FIG. 1. *P. syringae* pv. tomato DC3000 produces SA and Ybt under iron-limiting conditions. (A) Overlaid HPLC chromatograms showing SA extracted from iron-limited (black) and high-iron (gray) DC3000 cultures. Fluorescence at excitation of 305 nm and emission of 407 nm, optimal for SA, is shown. The structure of SA is shown in the upper right corner. (B) Overlaid HPLC chromatograms showing Ybt-Fe^{3+} with Ybt extracted from iron-limited (black) and high-iron (gray) DC3000 cultures, measured at a Ybt-Fe^{3+} absorbance maximum (385 nm). Extracted Ybt and Ybt-Fe^{3+} was saturated with Fe^{3+} prior to HPLC analysis to facilitate comparison. The absorbance profile of Ybt (at peak maximum, 17.8 min) is shown in the inset. (C) LC-MS (positive-ion mode) analysis of the DC3000 Ybt HPLC fraction. Black arrows indicate the major ion intensities (*m/z*) associated with the iron-bound monomer (*m/z*, 535.1 $[FeM+H]^+$), dimer (1,068.7), and trimer (1,603.5); gray arrows indicate dominant cleavage products. The structure of Ybt is shown in the upper right corner.

Bacterial growth in planta. *Arabidopsis thaliana* var. Col-0 and *ics1-2* (*eds16-1*) *Arabidopsis* mutant (79) plants were grown for 5 weeks in a 12-h light/dark cycle with PAR of ~150 $\mu Em^{-2}\,s^{-1}$, and leaves were infiltrated with a 10 mM $MgSO_4$

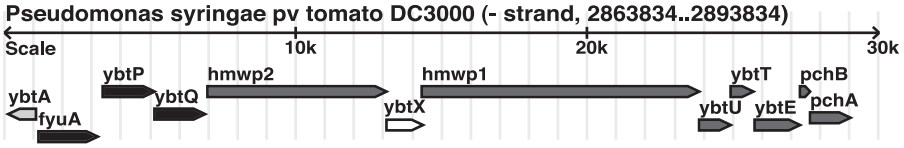

FIG. 2. Organization of the putative Ybt cluster in the genome of *P. syringae* pv. *tomato* DC3000. Gene names are modeled after the Ybt cluster in *Y. pestis*, except for *pchA* and *pchB*, which are named after the *P. aeruginosa* orthologs. *P. syringae* pv. tomato DC3000 genes from PSPTO2595 (*pchA*) to PSPTO2606 (*ybtA*) are shown. *ybtA* is shaded light gray and is an AraC-type transcriptional regulator. Transport genes are shaded black and consist of the TonB-dependent receptor *fyuA* and two ABC transporters, *ybtP* and *ybtQ*. Biosynthetic genes are shaded dark gray and include the isochorismate synthase gene *pchA* and the salicyl-AMP ligase gene *ybtE*. *ybtX* is shaded white and has no identified function in *Y. pestis*.

solution containing 5×10^5 CFU/ml of DC3000 strains. Mature leaves (trimmed to 1 cm^2) were then collected at 0, 1, or 3 days in 1 ml of 10 mM $MgSO_4$ and ground with a plastic pestle. Appropriate dilutions were then plated with a spiral plater (model D; Spiral Systems Instruments, Inc., Bethesda MD) on KB agar plates with 100 μg/ml rifampin and 15 μg/ml natamycin (fungicide), and bacterial colonies were counted with a laser colony counter (model 500A; Spiral System Instruments, Inc.). Tomato variety Bonny Best plants were grown for 6 weeks in a greenhouse and vacuum infiltrated with 10 mM $MgSO_4$ containing 5×10^5 CFU/ml of DC3000 wild-type or mutant strains. Leaflets of approximately 0.5 g (fresh weight) were ground in 1 ml of 10 mM $MgSO_4$ solution at 0 and 3 days. Plating and counting of colonies was performed as with *Arabidopsis*. Data are reported as means and standard deviations of three replicates. Complete experiments were performed twice with similar results.

RNA isolation and RT. RNA was collected from 5×10^8 CFU of liquid cultures using an RNeasy mini kit (QIAGEN) and DNase (QIAGEN) treated according to the manufacturer's instructions. cDNA was synthesized from 1 μg of RNA using a QuantiTect reverse transcription (RT) kit (QIAGEN) according to the manufacturer's instructions. Negative-control reactions lacked only reverse transcriptase. Resultant cDNAs were used in quantitative PCR (qPCR) experiments.

qPCR. cDNA samples were used as a template for qPCR of *pchA*, *ybtE*, and *pvdA*. PCR efficiencies for the different primer sets were determined to be comparable. PCR was performed with a QuantiTect SYBR green PCR kit (QIAGEN) and an ABI PRISM 7700 real-time cycler (ABI); 50-μl reactions were prepared according to the manufacturer's instructions using 50 ng of template cDNA. The primers used for the real-time reactions were 5′-CAGTTGC TTCATGGGTGCAT-3′ and 5′-GCCATGGTGTGCAATTGATC-3′ for *ics*, 5′-GCAGGTGACCGGGTCATG-3′ and 5′-GCAAACAATGCGCAGACAAA-3′ for *ybtE*, 5′-GGCGATGTTCGAATTCAACA-3′ and 5′-CCGCCAAGGCTTT CAAGA-3′ for *pvdA*, and 5′-CGCTAGTAATCGCGAATCAGAA-3′ and 5′-G ACGGGCGGTGTGTACAAG-3′ for 16S rRNA. Gene expression was normalized to 16S rRNA for each sample. Complete experiments were performed twice with similar results.

RESULTS

Synthesis of SA and Ybt by *P. syringae* pv. tomato DC3000. In order to determine whether *P. syringae* pv. tomato DC3000 synthesizes SA and Ybt, wild-type DC3000 was grown under high-iron (with 50 μM Fe^{3+}) or low-iron (iron-limited) conditions. As shown in Fig. 1, SA and Ybt are produced by DC3000 and detected in culture supernatant when grown under iron-limiting conditions. We routinely analyze SA in our laboratory by HPLC (70), and the SA chromatographic peak was confirmed by its fluorescence at excitation of 305 nm/emission of 407 nm and retention time compared with SA standards. Ybt was confirmed by comparing its iron-bound absorbance spectrum, retention time, ESI-MS positive-ion analysis (Fig. 1B and C), and MS-MS fragmentation (data not shown) with a Ybt standard and published results (12, 26, 40, 58, 59). Similar to published results for Ybt isolated from other bacterial species or strains, we observed a major ion intensity at *m/z* of 535.1 $[FeM+H]^+$ for iron-saturated Ybt-Fe^{3+} and a minor ion intensity at *m/z* of 348.9 corresponding to the Ybt 295 cleavage product + Fe. This Ybt 295 cleavage product results from the loss of an uncharged 186 fragment (26). In addition, major ion intensities associated with the Ybt-Fe^{3+} dimer (*m/z* = 1,068.7), the dimer −186 fragment (*m/z* = 882.9), and the Ybt-Fe^{3+} trimer (*m/z* = 1,603.5) were also observed, in agreement with previous reports (12, 26). This is, to our knowledge, the first reported detection of SA and Ybt produced by the well-studied plant pathogen *P. syringae* pv. tomato DC3000.

DC3000 synthesis of SA and Ybt requires the isochorismate synthase *pchA*. The isochorismate synthase *pchA*, responsible for the conversion of chorismate to isochorismate, is required for the synthesis of SA and SA-derived siderophores in well-characterized species such as *Pseudomonas aeruginosa* PAO1 (67, 68). The genes responsible for SA synthesis from chorismate in DC3000 are included in the Ybt biosynthetic cluster (Fig. 2). Therefore, to confirm that the predicted DC3000 Ybt biosynthetic cluster is responsible for the Ybt and SA detected in our iron-limited cultures, we created a *pchA* (PSPTO2595) insertion mutant of DC3000. As expected, SA and Ybt production were abrogated in the DC3000 *pchA* mutant (Fig. 3). To determine whether downstream Ybt biosynthetic enzymes were still expressed, translated, and assembled into a functional complex, we supplemented iron-limited medium with 10 μM SA. This supplementation restored Ybt production in the *pchA* mutant (data not shown).

Impact of SA and Ybt on DC3000 growth and virulence in plant hosts. As *Pseudomonas syringae* pv. *tomato* DC3000 is pathogenic on tomato and *Arabidopsis*, we tested whether the

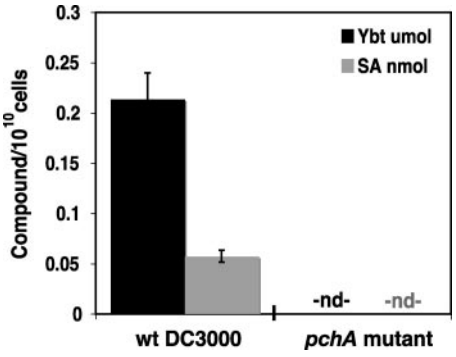

FIG. 3. Synthesis of SA and Ybt requires a functional *pchA* gene. Shown are SA (gray) and Ybt (black) measured in iron-limited culture supernatants at 24 hpi with wild-type (wt) *P. syringae* pv. tomato DC3000 or the *pchA* DC3000 mutant. The DC3000 *pchA* mutation is in the isochorismate synthase gene of the putative Ybt biosynthetic cluster. nd, not detected (below detection limit).

pchA mutant exhibited altered bacterial growth or disease-associated symptoms in these host plants. Intercellular *P. syringae* pathogens enter plant leaves through the stomata, multiply in the intercellular space (apoplast), and eventually produce visible disease symptoms (41). On susceptible tomato and *Arabidopsis* plants, *P. syringae* pv. tomato DC3000 is virulent, with progressive bacterial growth and visible symptoms of disease, including gray-brown lesions with chlorosis spreading out from the lesions (77). Low-dose bacterial infiltration assays have been successfully used to identify individual components of bacterial virulence or plant resistance/susceptibility (e.g., (36). Therefore, we examined in planta bacterial growth and associated disease symptoms following infiltration of a low dose (OD_{600} = 0.0003) of wild-type DC3000 or *pchA* mutant strains into leaves of the susceptible hosts tomato var. Bonny Best and *Arabidopsis thaliana* Col-0. We observed no significant growth defect of the *pchA* mutant compared to *P. syringae* pv. tomato DC3000 wild-type strains in susceptible tomato or *Arabidopsis* hosts (Fig. 4A and B). Furthermore, we observed no visible differences in disease symptoms (data not shown). Initial bacterial colonization of the leaf surface and stomatal ingress can also play important roles in *P. syringae* virulence (7, 50). Therefore to assess whether the *pchA* mutant might have a defect in initial colonization or ingress, we sprayed wild-type and *pchA* mutant bacterial suspensions onto *Arabidopsis* Col-0 leaves. We observed no significant, reproducible difference in *Arabidopsis* disease symptoms following application with the mutant versus wild-type strains at standard (OD_{600}, 0.275) or high (OD_{600}, 1.0 or 2.0) sprayed doses (data not shown).

Tomato and *Arabidopsis* accumulate SA in response to pathogen infection as a key component of the plant defense response. In *Arabidopsis*, this pathogen-induced SA is synthesized from isochorismate (79). Isochorismate synthase *ics1* mutants in AtICS1 (At1g74710) exhibit enhanced disease susceptibility with abrogated pathogen-induced SA accumulation and SA-dependent pathogenesis-related gene expression (25, 54, 79). Though pathogen-induced SA appears to be synthesized in the plastid (70), it also accumulates in the apoplast. For example, using an SA biosensor strain, apoplastic free SA in tobacco increased from an undetectable level in untreated leaves to 6.5 μM at 16 hours postinoculation (hpi) with tobacco mosaic virus to levels as high as 81 to 380 μM in isolated sites associated with developing (40 hpi) or visible (90 to 168 hpi) hypersensitive response lesions (42). As discussed earlier, exogenous SA (10 μM) restored Ybt synthesis in the *pchA* mutant under iron-limiting conditions. Therefore, we wanted to determine whether apoplastic plant-produced SA could complement the DC3000 *pchA* mutation by providing SA for bacterial Ybt production, thus resulting in lack of an observable growth defect or altered disease symptoms. Inoculation of *ics1 Arabidopsis* plants with the *pchA* mutant resulted in no growth defect or altered disease symptoms (not shown) compared to DC3000 (Fig. 4C). Furthermore, there were no robust, reproducible differences in disease symptoms when wild-type or mutant bacterial strains were sprayed onto *ics1 Arabidopsis* plants (data not shown). As induced SA synthesis is abrogated in the *ics1 Arabidopsis* mutant and uninduced, constitutive leaf apoplastic SA levels appear to be extremely low (42), plant-produced SA is not likely to be responsible for the lack of a *pchA* phenotype in planta.

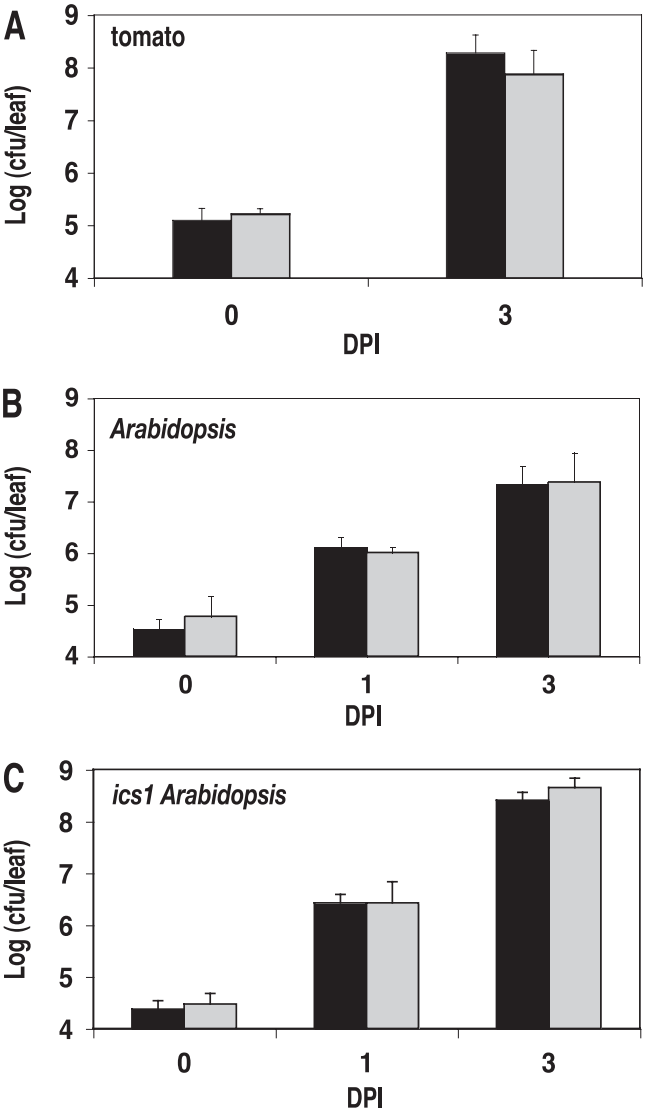

FIG. 4. In planta bacterial growth of *P. syringae* pv. tomato DC3000 and the *pchA* mutant. Bacterial growth in planta is shown for infection of susceptible plant hosts: tomato (A), *Arabidopsis thaliana* (B), and the *Arabidopsis ics1* mutant, which has a defect in the synthesis of pathogen-induced SA (C). Mature leaves of these plants were infiltrated with *P. syringae* pv. tomato DC3000 (black) or the *pchA* mutant (gray) at a dose of 5×10^5 CFU/ml. In planta bacterial growth was assessed at 0, 1, and 3 dpi.

The enhanced growth of both the *pchA* and wild-type *P. syringae* pv. tomato DC3000 strains in the *ics1* mutant compared with wild-type *Arabidopsis* is consistent with previous results and the role of plant-produced SA in limiting pathogen growth (54). As the DC3000 and *pchA* mutant strains both exhibited similarly enhanced growth (~1 $\log_{10}$ at 3 days postinoculation [dpi]) on the *ics1* mutant compared with wild-type *Arabidopsis* in side-by-side experiments, our results also indicate that SA produced by *P. syringae* pv. tomato DC3000 cannot compensate for the lack of pathogen-induced plant-produced SA in the *ics1 Arabidopsis* mutant.

Ybt is produced by *P. syringae* pv. tomato DC3000 in planta. Given our lack of growth or altered disease phenotype for the

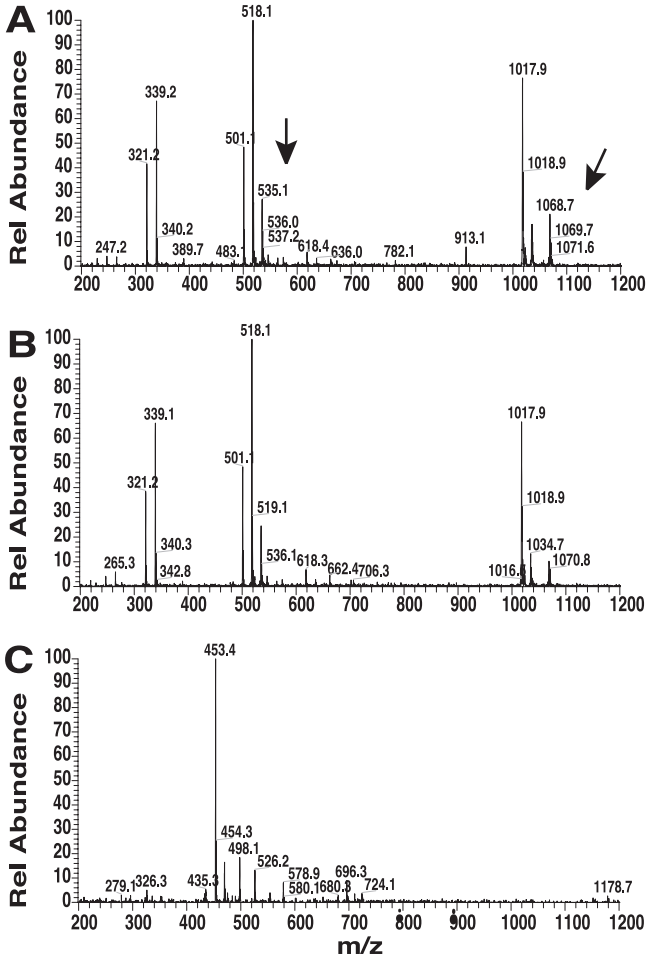

FIG. 5. Detection of Ybt in planta. LC-MS analysis of Ybt from *Arabidopsis* leaf extracts harvested 5 dpi with *P. syringae* pv. tomato DC3000 (A), the *pchA* mutant (B), or control treatment (10 mM $MgS0_4$) (C). ESI (positive ion) of 200 to 1,200 for the elution time of Ybt-Fe^{3+} is shown. Major ion intensities (*m*/*z*) for the iron-bound Ybt monomer (*m*/*z*, 535.1; dimer, 1,068.7) are indicated with an arrow where present.

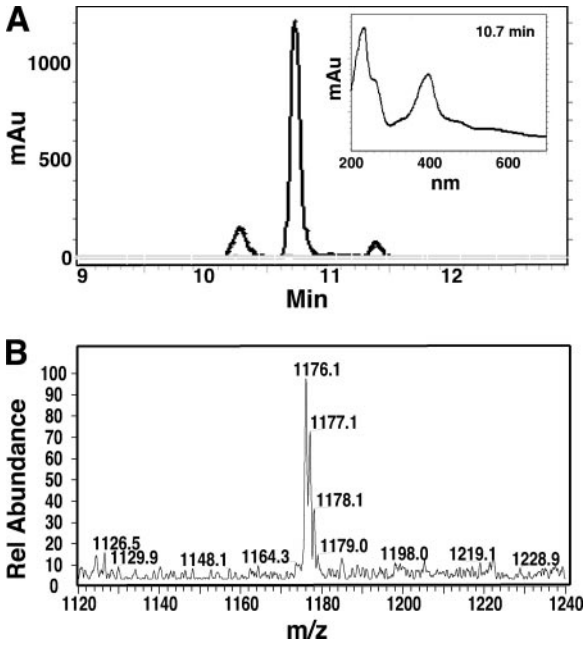

FIG. 6. Production of Pvd by *P. syringae* pv. tomato DC3000. (A) HPLC chromatogram showing Pvd peaks, measured by absorbance at 400 nm for culture extracts isolated from iron-limited cultures (black) or high-iron cultures (gray). The absorbance profile of the dominant Pvd peak at its maximum (10.7 min) is shown in the inset. (B) LC-MS (positive-ion mode) analysis of the DC3000 dominant Pvd HPLC fraction. The relative abundance of the major ion intensities (*m*/*z*) from 1,120 to 1,240 is shown.

pchA mutant on susceptible plant hosts, we sought to determine whether Ybt was produced by *P. syringae* pv. tomato DC3000 in planta. We were not able to specifically examine SA produced by DC3000 in planta, as our estimates for SA produced by DC3000 (<1 pmol SA/leaf, assuming in planta SA production similar to that of iron-limited cultures [e.g., see Fig. 3]) are well below the uninduced levels of free SA produced by *Arabidopsis*.

To determine whether Ybt was produced in planta, we extracted DC3000 and *pchA* mutant-infected *Arabidopsis* leaves at 5 dpi, analyzed these samples by HPLC, and collected the putative Ybt fractions based on Ybt retention time. The samples were then analyzed by ESI-MS and compared with our ESI-MS results from Ybt extracted from culture supernatant (Fig. 1C). The dominant Ybt ions (*m*/*z*, 535.1 [monomer]; *m*/*z*, 1,068.7 [dimer]) were detected in extracts from DC3000-sprayed plants but not in extracts from plants sprayed with the *pchA* mutant or a buffer control (Fig. 5). Furthermore, MS-MS fragmentation of the 535 ion of the DC3000-infected *Arabidopsis* leaf sample resulted in an essentially identical fragmentation pattern to that for MS-MS analysis of Ybt extracted from DC3000 culture supernatants (data not shown). We observed production of both the −186 Ybt fragment of *m*/*z* 349, as described previously (26), and the *m*/*z* 489 ion thought to arise from decarboxylation of the molecular ion of the FeH^+ adduct (12, 58). These results indicate that (i) Ybt is synthesized by *P. syringae* pv. tomato DC3000 during its infection of *Arabidopsis*, (ii) synthesis of Ybt in planta requires a functional DC3000 *pchA* gene, and (iii) plant-derived SA is unable to restore bacterial Ybt production in the *pchA* mutant.

Synthesis of the siderophore Pvd by *P. syringae* pv. tomato DC3000 may mask the functional role of Ybt. In phytopathogens synthesizing multiple high-affinity siderophores, the inability to synthesize a single siderophore may not result in an observable growth or disease phenotype depending on the pathosystem (e.g., (19). In some cases, the inability to produce one siderophore results in altered compensatory production of the other siderophore(s), as observed for *D. dadantii* in culture (34). In addition to Ybt, *P. syringae* pv. tomato DC3000 likely synthesizes the yellow-green fluorescent siderophore Pvd, based on the presence of the required biosynthetic genes in its genome (11) and the synthesis of Pvd by other *P. syringae* pv. tomato strains (13, 14). Therefore, we first wanted to determine whether DC3000 produces Pvd under iron-limiting conditions. As shown in Fig. 6A, Pvd was produced by *P. syringae* pv. tomato DC3000 under iron-limiting conditions, with significant enrichment compared to its levels in iron-rich culture supernatants. The identity of Pvd was confirmed by its absor-

bance spectrum and by ESI-MS (Fig. 6A and B). Its specific spectral traits and size (molecular weight, 1,175) indicate that it is similar to the atypical Pvd characterized as the dominant Pvd of *Pseudomonas syringae* pv. syringae B301D (18) and present in numerous *Pseudomonas syringae* strains, including *P. syringae* pv. tomato LMG5093 (13, 15). This Pvd_{pss} contains the 2,3-diamino-6,7-dihydroxy-quinoline chromophore characteristic of all Pvd in addition to a heptapeptide consisting of two β-hydroxyaspartic acids, two serines, two threonines and one lysine (18). This is, to our knowledge, the first reported detection and characterization of the *P. syringae* pv. tomato DC3000 Pvd.

Impact of increasing dipyridyl on Ybt and Pvd production by *P. syringae* pv. tomato DC3000 and the *pchA* mutant. As the relative production of the siderophores of a given phytopathogen can differ depending on the amount of available Fe^{3+}, we first assessed the production of Ybt and Pvd by *P. syringae* pv. tomato DC3000 in cultures grown with progressively more limiting amounts of Fe^{3+}. As shown in Fig. 7, growth of DC3000 is significantly impacted as available iron is limited by increasing dipyridyl concentrations. Total Ybt and Pvd in culture supernatants were highest at low levels of dipyridyl; however, when siderophore levels were normalized on a cell basis, they increased with progressive iron limitation (Fig. 7A and B). We observed no preferential synthesis of Ybt versus Pvd (or vice versa) for any part of the iron limitation regimen (0 to 200 μM dipyridyl).

To determine whether Pvd may compensate for lack of Ybt production in the *pchA* mutant, we first compared growth of wild-type DC3000 and the *pchA* mutant in culture under progressively limited Fe^{3+} conditions (as above). A simple expectation was that if Pvd was unable to compensate for Ybt, we might observe reduced growth for the *pchA* mutant, particularly under more stringent iron-limiting conditions (e.g., 150 to 200 μM dipyridyl). Alternatively, if Pvd could compensate for Ybt absence in the *pchA* mutant, we would expect to see no difference in growth between the wild-type and mutant strains. Surprisingly, as shown in Fig. 7C, we found enhanced growth of the *pchA* mutant compared with that of the wild type, with a greater relative increase in *pchA* growth compared to that of the wild type as available iron is more limited (i.e., with higher dipyridyl concentrations).

As no growth defect (and in fact an enhancement) was observed for the *pchA* mutant as iron was progressively more limited, we determined whether Pvd production was altered in the *pchA* mutant compared with the wild type. We observed enhanced Pvd in culture supernatants of the *pchA* mutant compared with the wild type with increasing dipyridyl (Fig. 7D). However, the *pchA* mutant also grew better than the wild type under these conditions (Fig. 7C), and cell-normalized Pvd levels are not significantly higher in the *pchA* mutant than in the wild type. In the experiment presented in Fig. 7D, it appears that there may even be less Pvd on a cell basis in the *pchA* mutant than in the wild type at 150 and 200 μM dipyridyl; however, repeated experiments indicate that cell-normalized Pvd is not significantly different for the wild type and the mutant.

Conditional experiments under stringent iron limitation (150 μM dipyridyl). Because we saw no growth defect in the *pchA* mutant in planta (Fig. 4) or in the *pchA* mutant in culture under conditions of progressive iron limitation (Fig. 7C), we assessed whether the *pchA* mutant might exhibit a growth defect in culture under a variety of physiologically relevant conditions (Fig. 8). These conditional experiments were performed as described above but with variation in our standard temperature, pH, and redox conditions.

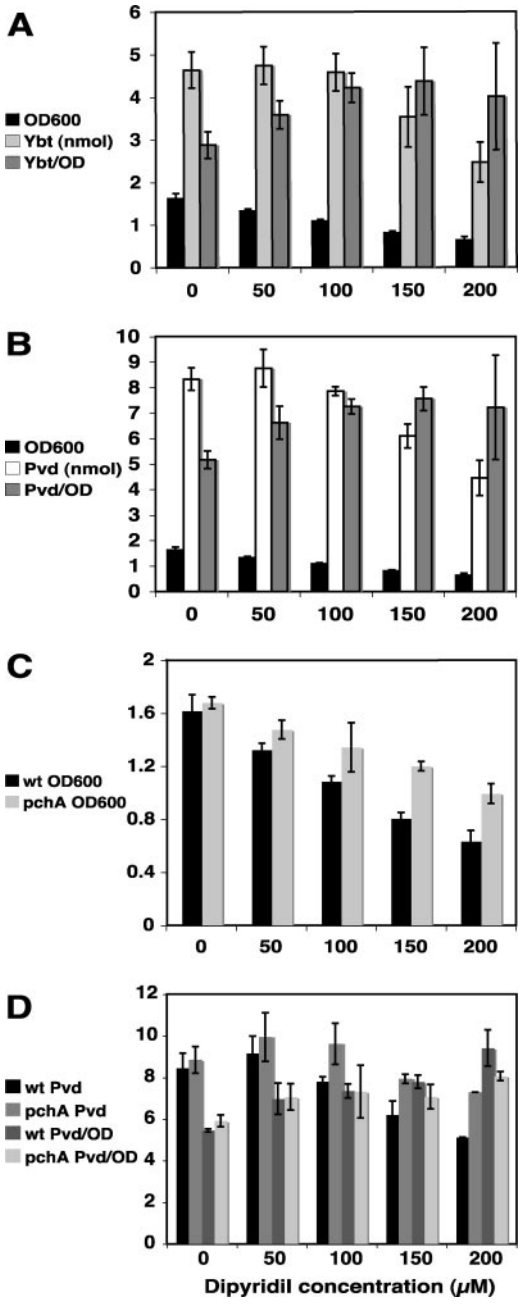

FIG. 7. Bacterial growth and siderophore production in culture as iron is progressively more limited through the addition of 2,2-dipyridyl. Siderophores were measured in culture supernatants at 24 hpi. (A) *P. syringae* pv. tomato DC3000 growth (OD_{600}) and Ybt production (nmol). (B) *P. syringae* pv. tomato DC3000 growth (OD_{600}) and Pvd production (nmol). (C) Growth (OD_{600}) of *P. syringae* pv. tomato DC3000 compared with that of the *pchA* mutant. (D) Pvd production (nmol) by *P. syringae* pv. tomato DC3000 compared with that of the *pchA* mutant.

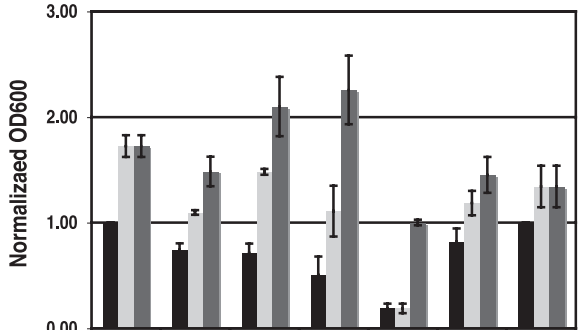

	20 C	30 C	1 mM DTT	5 mM H2O2	pH 5.7	pH 6.5	pH 7.2
wt	1.00	0.74	0.71	0.51	0.19	0.82	1.00
pchA	1.73	1.10	1.48	1.11	0.19	1.19	1.34
pchA/wt	1.73	1.49	2.10	2.26	1.00	1.45	1.34

FIG. 8. Conditional experiments varying temperature, redox conditions, and pH show enhanced growth of the *pchA* mutant compared with Pst DC3000 under stringent iron-limiting conditions. Bacterial growth (OD_{600}) was assessed for cultures at 24 hpi under iron-limiting conditions (with 150 μM dipyridyl) with varying levels of temperature, oxidant (H_2O_2), reductant (DTT), or pH to assess differences in bacterial growth under potentially environmentally relevant conditions. Data are normalized to growth of DC3000 under standard conditions (20°C, pH 7.2).

Plant leaf temperature is not tightly moderated and can be expected to vary regularly in the field. Our *Arabidopsis* plants are grown in a controlled growth chamber at 22°C, and our standard assay in culture has been performed at 20°C. Perhaps SA and Ybt production and function are important for maximal growth at high temperatures, resulting in a growth defect in the *pchA* mutant at 30°C but not 20°C. As shown in Fig. 8, we found that the *pchA* mutant still exhibited enhanced growth relative to wild-type *P. syringae* pv. tomato DC3000 at 30°C. In iron-rich medium, DC3000 typically exhibits higher growth at 30°C than at 20°C. In contrast, we found that in iron-limited medium both the wild type and the *pchA* mutant exhibited enhanced growth at 20°C but not at 30°C. This is perhaps due to enhanced iron acquisition resulting from higher total and cell-normalized Ybt and Pvd production at 20°C (data not shown).

In addition to differing temperatures, pathogens in the leaf apoplast may also experience changes in reducing or oxidizing (redox) conditions. Plants produce reactive oxygen species in addition to SA as part of the immune response to pathogens, including oxidants such as H_2O_2 (24). Reductant concentrations can also vary as a function of environmental conditions, including light, temperature, abiotic stress, and pathogen attack (10). Therefore, we examined growth of DC3000 and the *pchA* mutant under more oxidizing (additional H_2O_2) or reducing (additional DTT) conditions in culture. Though H_2O_2 and DTT negatively impacted the growth of both strains, once again the *pchA* mutant exhibited enhanced growth compared to the wild type (Fig. 8). Indeed, the relative growth of *pchA* compared with the wild type was reproducibly higher under these conditions than under any other condition tested.

pH has been shown to impact bacterial growth and siderophore production (72). It also has a dramatic impact on the affinity of siderophores for iron, with differential impacts on distinct siderophores (72). Therefore, we were interested in determining the influence of pH on the growth of the *pchA* mutant versus that of the wild type to determine whether Ybt plays a greater functional role at a pH other than 7.2 (our standard conditions). At pH 7.2, Ybt is likely to have a higher affinity for Fe^{3+} than Pvd, as pFe Ybt is 10^{36} at pH 8.5 (58) and pFe Pvd is 10^{32} at pH 10, with decreasing affinity at lower pHs (i.e., pFe Pvd is 10^{25} at pH 7) (18). The plant apoplast is more acidic than our standard pH, with typical values ranging from pH 5.3 to 6.7 (see, e.g., reference 35). In *Arabidopsis*, a resting apoplastic pH of 6.3 was reported (35), and environmental stresses can alter apoplastic pH significantly (i.e., by 1 to 1.5 pH units [31]). Therefore, we tested the growth of DC3000 and the *pchA* mutant at pH 5.7, 6.5, and 7.2. Though lower pH resulted in reduced growth for both strains, we did not observe a significant growth defect in the *pchA* mutant compared to the wild type (Fig. 8). At pH 6.5, the *pchA* mutant exhibited enhanced growth compared to the wild type, similar to that at pH 7.2. At pH 5.7, bacterial growth of both strains was severely compromised, with fivefold-lower growth than at pH 7.2. This could be due to ineffective iron acquisition, as both Pvd and Ybt are predicted to be dramatically less effective at binding Fe^{3+} at lower pHs (18, 72).

In summary, under all conditions tested with stringent iron limitation (150 μM dipyridyl), the *pchA* mutant exhibited enhanced growth compared with that of the wild type.

Siderophore production under low-iron conditions. As discussed above, as iron was progressively less available (50 to 200 μM dipyridyl), the *pchA* mutant exhibited increasingly enhanced growth compared to wild-type *P. syringae* pv. tomato DC3000. Levels of potentially available iron in the leaf apoplast can range from 1.6 μM to 6 μM, with the lower values being associated with iron deficiency (48, 49). Therefore, we decided to examine relative growth of the wild type versus the *pchA* mutant as we added progressively more iron (e.g., from 0 to 50 μM $FeCl_3$). Unlike our findings when dipyridyl was added to the culture medium, we found that the wild-type and *pchA* mutant strains exhibited similar growth when 0 to 50 μM of $FeCl_3$ was added. At 10 μM added $FeCl_3$, iron no longer limited growth and we observed a fivefold increase in growth in both strains that was consistent from 10 to 50 μM $FeCl_3$ (data not shown). In both the added-dipyridyl and added-iron experiments, the wild-type and *pchA* mutant strains grew similarly with no added dipyridyl or iron. Therefore, we decided to further examine the role of Ybt and Pvd under a low-iron condition in which bacterial growth is still partially limited and siderophores are produced but mutant and wild-type DC3000 strains exhibit similar growth.

As shown in Fig. 9A, under this low-iron condition, both Ybt and Pvd are detected in the *P. syringae* pv. tomato DC3000 culture supernatant by 10 h. Pvd levels increase with time through the 48-h time course, whereas Ybt levels peak at 24 h with ~90% of maximal Ybt at 48 h. Through this time course, the wild-type DC3000 and *pchA* mutant strains grew equally well (Fig. 9B). To determine whether enhanced Pvd levels in the *pchA* mutant might compensate for the loss of SA and Ybt synthesis, we measured Pvd in culture supernatants of DC3000 versus *pchA* mutant through this time course. To our surprise, we found reduced Pvd in culture supernatants of the *pchA* mutant (Fig. 9C). In total, these results suggest that Ybt is not required for growth under these low-iron conditions. Further-

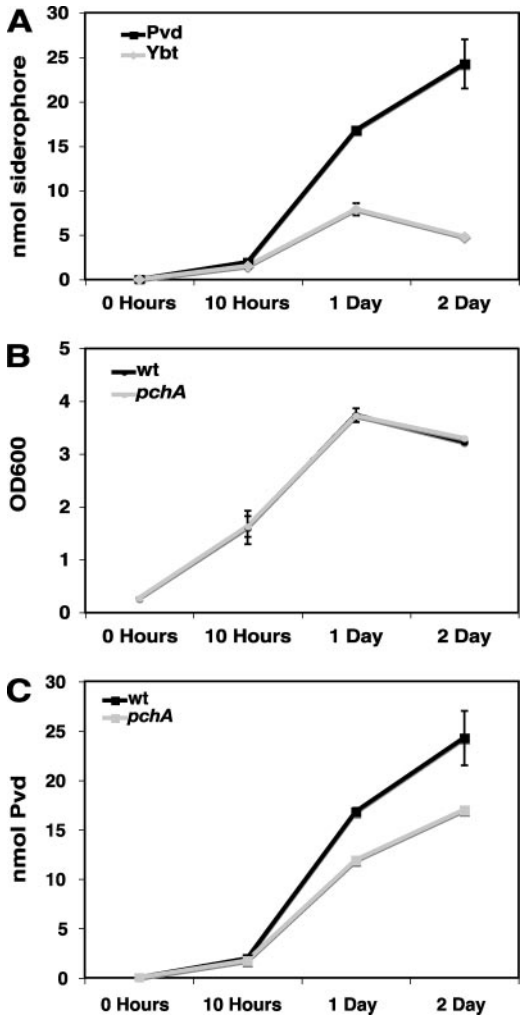

FIG. 9. Time course of growth and siderophore production by *P. syringae* pv. tomato DC3000 and the *pchA* mutant under low-iron conditions. (A) Pvd and Ybt levels in culture supernatants of *P. syringae* pv. tomato DC3000. (B) Growth curve for *P. syringae* pv. tomato DC3000 and the *pchA* mutant. (C) Pvd levels in culture supernatants of DC3000 or the *pchA* mutant. Low-iron conditions are equivalent to no added dipyridyl or added $FeCl_3$.

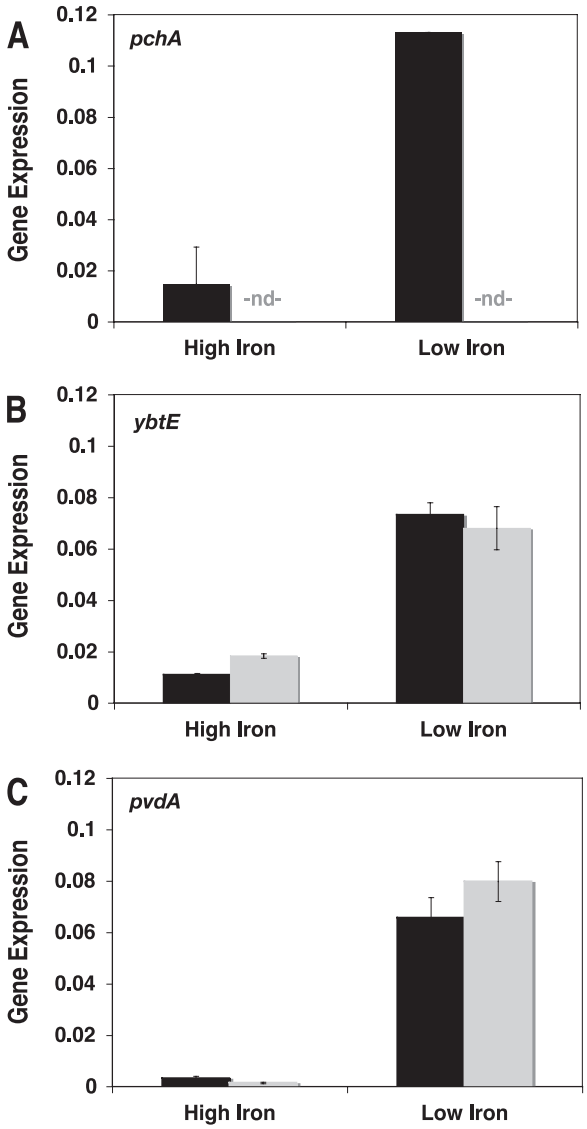

FIG. 10. Expression of SA, Ybt, and Pvd biosynthetic genes by DC3000 and the *pchA* mutant in high-iron or low-iron cultures. Shown is normalized expression of *pchA* (A), *ybtE* (B), and *pvdA* (C) in wild-type *P. syringae* pv. tomato DC3000 (black) and the *pchA* mutant (gray) at 24 hpi in high-iron (with 50 μM $FeCl_3$) or low-iron medium. *pchA* (PSPTO2595) is required for SA and Ybt biosynthesis. *ybtE* (PSPTO2597) is required for Ybt biosynthesis from SA. *pvdA* (PSPTO2135) is required for Pvd biosynthesis. RNA isolation and qPCR were performed as described in Materials and Methods. Gene expression was normalized to 16S rRNA for each sample and multiplied by 1,000 for ease of presentation. nd, not detected (below detection limit).

more, it appears that excreted Pvd in DC3000 is more than sufficient to bind available iron in the medium, as a 30% reduction in Pvd in the culture supernatant of the *pchA* mutant did not compromise its growth.

Expression of siderophore biosynthetic genes. To explore the regulation of siderophore biosynthesis in *P. syringae* pv. tomato DC3000, we performed qPCR to assess the expression of the Ybt biosynthetic genes *pchA* (PSPTO2595; the isochorismate synthase required for the synthesis of SA) and *ybtE* (PSPTO2597; the salicyl-AMP ligase required for the synthesis of Ybt from SA) and the Pvd biosynthetic gene *pvdA* (PSPTO2135; a peptide synthase required for the synthesis of the Pvd chromophore (53). As expected, *pchA*, *ybtE*, and *pvdA* were not expressed by DC3000 under high-iron conditions (50 μM $FeCl_3$) but were expressed under low-iron conditions (as above) for 24 h (Fig. 10).

We then compared expression of these genes in the wild-type versus *pchA* mutant strains. As the *pchA* mutant contains an insertion in the *pchA* gene, *pchA* was not expressed in the *pchA* mutant (Fig. 10A). *ybtE* was expressed similarly to DC3000 in the *pchA* mutant under low-iron conditions (Fig. 10B). The induced expression of *ybtE* in the *pchA* mutant was surprising, as maximal expression of siderophore biosynthetic genes in similar characterized systems typically involves a siderophore-dependent amplification (e.g., Ybt in *Yersinia enterocolitica* [4] and *Y. pestis* [6] and pyochelin in *P. aeruginosa* [52,

64]). We then compared *pvdA* expression in DC3000 versus the *pchA* mutant. As 70% of wild-type Pvd levels are measured in culture supernatants of the *pchA* mutant at 24 h compared with the wild type under these conditions, *pvdA* expression might also be reduced in the *pchA* mutant. In two separate experiments, we observed *pvdA* expression in the *pchA* mutant to be 85% and 82% of wild-type levels by qPCR (Fig. 10C). However, as this difference is within the standard deviation associated with each experiment, we can conclude only that there is no dramatic difference in *pvdA* expression in the *pchA* mutant.

DISCUSSION

Herein, we characterize the iron-regulated siderophore production of the well-studied plant pathogen *P. syringae* pv. tomato DC3000 and demonstrate, for the first time, that SA, Ybt, and an atypical Pvd (Pvd_{pss} [18]) are produced by DC3000 when iron is limited. We show that SA and Ybt synthesis in DC3000 is dependent on the isochorismate synthase gene *pchA* through analysis of a *pchA* insertion mutant and establish that SA is a required precursor for Ybt synthesis. Using this *pchA* mutant, we explored the functional importance of SA and Ybt in culture and in pathogenesis. We determined that DC3000 produces Ybt in the course of infection in planta and that this production requires *pchA*. However, we did not observe any differences in bacterial growth or visible disease symptoms of plants infected with the *pchA* mutant versus wild-type *P. syringae* pv. tomato DC3000. To determine whether *pchA* might be required for initial leaf colonization and bacterial ingress through plant stomata or wounds, we also assessed the plant virulence phenotype in response to the spraying of bacterial cultures onto the leaf surface. No virulence difference was observed in plant leaves sprayed with the *pchA* mutant compared with wild-type DC3000.

Role of Ybt in *P. syringae* pv. tomato DC3000 pathogenesis. As Ybt is synthesized by *P. syringae* pv. tomato DC3000 in planta, why did the *pchA* mutant exhibit no fitness or virulence defect? Possible explanations include (i) the *pchA* mutant utilizes plant-produced SA to make Ybt, (ii) the DC3000 siderophore Pvd is able to functionally compensate for loss of Ybt production under these conditions, or (iii) under the conditions tested, Ybt or high-affinity siderophores in general are not required for bacterial virulence in planta.

We addressed the first possibility experimentally by assessing whether the *pchA* mutant exhibited a growth or disease phenotype when inoculated or sprayed onto the SA biosynthetic mutant *ics1*. If plant-produced SA restored *pchA* Ybt formation in wild-type plants, then the *ics1* mutant would be unable to restore Ybt production and a growth defect for the *pchA* mutant would be observed on the *ics1* mutant plants. Instead, no growth difference was observed for the *pchA* mutant versus DC3000 on the *ics1* plants. We then confirmed this directly by examining in planta Ybt production. Whereas Ybt was detected in *Arabidopsis* leaf extracts infected with DC3000, it was not detected in *pchA*-infected leaf extracts. Thus, under the conditions examined, plant-produced SA does not rescue the *pchA* mutation. This finding might also suggest that *P. syringae* pv. tomato exposure to *Arabidopsis* SA is low ($\ll$10 μM) in this virulent interaction, in contrast to experiments demonstrating higher apoplastic SA in an avirulent interaction (42).

To address the second explanation for the lack of a virulence defect for the *pchA* mutant (i.e., Pvd compensates for lack of Ybt production), we undertook a series of experiments. We were first interested in determining whether there were conditions under which Ybt was preferentially synthesized over Pvd by DC3000. We examined Ybt and Pvd production (assessed from culture supernatants) as iron was progressively more limited (through the addition of 2,2′-dipyridyl), progressively more available (with added $FeCl_3$), under a variety of relevant environmental conditions (acidic pH, redox stress, temperature stress), and over time. Generally, Pvd and Ybt levels were correlated and of a similar magnitude, with Pvd typically 1.5- to 2-fold higher on a nanomolar basis. However, the low-iron time course experiment showed that while Ybt and Pvd accumulate similarly in early cultures, over time Pvd becomes the more prevalent siderophore (Fig. 9A). Indeed, at the late stationary phase time point (48 h), Pvd levels continue to increase while Ybt decreases. This difference in Pvd versus Ybt is not likely due to increased iron limitation, as this pattern is not observed with increasing dipyridyl (Fig. 7), but may be due to differential regulation or utilization (discussed below). We also examined growth of the *pchA* mutant versus the wild type in the above experiments and found that the mutant grew similarly to wild-type DC3000 under iron-rich or low-iron conditions but exhibited enhanced growth under more stringent iron-limiting conditions (i.e., with added dipyridyl).

In the phytopathogen *D. dadantii* 3937, chrysobactin or achromobactin biosynthetic mutants partially compensate for loss of one siderophore by compensatory changes in the timing and amount of the remaining siderophore produced under iron-limiting conditions in vitro (34). Therefore, we were interested in determining whether we would see enhanced Pvd in culture supernatants of the *pchA* mutant to compensate for lack of Ybt production. This does not seem to be the case. Under stringent low-iron conditions in which the *pchA* mutant grows better than wild-type DC3000, the *pchA* mutant does overproduce Pvd but not on a cell-normalized basis. In fact, under conditions in which the two strains grow similarly, the *pchA* mutant produces less Pvd than does the wild type. For example, though the *pchA* mutant and DC3000 grew equally well in the low-iron time course experiment (Fig. 9), Pvd levels for the *pchA* mutant were less than those of the wild type throughout the time course (10 to 48 h). This suggests that for the *pchA* mutant, the available Pvd (~70% of that for the wild type) was sufficient to supply the iron needed for growth. In summary, under the conditions tested, Pvd is synthesized with Ybt and could alone be sufficient for iron acquisition in vitro and therefore in planta.

As mentioned above, it is also possible that high-affinity siderophores are not required for *P. syringae* pv. tomato DC3000 iron acquisition in the plant apoplast under the growth and environmental conditions assessed, thereby resulting in no virulence defect for the *pchA* mutant. Published values for Fe^{3+} in the leaf apoplast range from 1.6 to 6 μM Fe^{3+} with the iron complexed predominantly by citrate (9, 48, 49). *P. syringae* pv. tomato DC3000 contains a putative FecA ferric dicitrate transporter (PSPTO1207). As most bacteria require 10^{-6} to 10^{-7} M levels of bioavailable iron for optimal growth (39), it is possible that ferric citrate alone could provide sufficient iron for bacterial growth in the leaf apoplast. This can

be compared to mammalian pathogens such as PAO1, which can import host iron-binding compounds such as heme to overcome the minute levels of available Fe^{3+} in mammalian biological fluids, estimated to be less than 10^{-18} M (38, 60, 78).

Future work with a Ybt$^-$ Pvd$^-$ biosynthetic *P. syringae* pv. tomato DC3000 double mutant should enable us to assess the above possibilities. If Pvd functionally compensates for lack of Ybt production in the *pchA* mutant, then the double mutant should show severely compromised growth in planta. If reduced growth is not observed in the double mutant, then, under these conditions, neither high-affinity siderophore is required.

Ybt is not required for optimal bacterial growth or virulence under the tested environmental and assay conditions but may still play an important role under more ecologically relevant conditions. For example, in our experiments, plants were grown in controlled environments where environmental stresses such as temperature fluctuations, drought, and dramatic changes in light intensity did not occur. In addition, our plants were grown under standard conditions without mineral or nutrient limitation. Finally, these plants were not exposed to the typical suite of interactors: other pathogens, symbionts, and pests. Therefore, the synthesis of SA and Ybt by *P. syringae* pv. tomato DC3000 may still confer a benefit in colonizing the leaf surface or apoplast in a field setting. In addition, we examined compatible interactions in which DC3000 is virulent on the susceptible plant host and programmed cell death associated with avirulent hypersensitive response is not elicited. It is possible that Ybt production by *P. syringae* pv. tomato DC3000 is beneficial in the context of a robust plant immune response, as apoplastic SA accumulation appears to be significantly higher in response to avirulent pathogens (>100 μM [42]). As there is the potential for these levels of apoplastic SA to be cytotoxic and to have a role in activating defenses, the ability of DC3000 to utilize this SA in Ybt synthesis could confer additional benefits.

To elucidate growth conditions under which Ybt contributes to fitness, we carried out a series of bacterial growth experiments in culture. We examined conditions of progressive iron limitation and additional stresses associated with the leaf apoplast such as oxidative stress, acidic pH, and temperature stress. Surprisingly, we found that the *pchA* mutant exhibited enhanced growth compared with wild-type DC3000 as iron was progressively more limited and with these additional stresses. This growth advantage conferred by the *pchA* mutation compared with the wild type in stringent iron-limited culture suggests that Ybt biosynthesis can be detrimental. The effect has at least three nonexclusive explanations. First, if Pvd production is sufficient for maximal iron acquisition under these conditions, then the *pchA* mutant would have enhanced growth due to the elimination of an unnecessary metabolic cost. Second, if Pvd is the more effective iron scavenger under these conditions and Ybt production interferes with Pvd function, then the *pchA* mutant would have enhanced growth when iron is most limited and Pvd function most critical. Third, if Ybt (and/or SA) has a role independent of iron acquisition that results in decreased fitness under these conditions, then the *pchA* mutant would have enhanced growth due to release from this effect.

We did not find previous reports of enhanced growth of a high-affinity siderophore biosynthetic mutant under iron-limiting conditions. However, it is widely acknowledged that loss of virulence factor production is associated with enhanced fitness for bacteria grown in culture where these factors do not provide sufficient benefit. In addition, fitness costs are associated with the production of biosynthetically complex secondary metabolites such as antibiotics when their synthesis provides no competitive advantage; therefore, their synthesis is typically finely regulated (see, e.g., reference 20). In terms of assessing the relative cost of Ybt versus Pvd use by *P. syringae* pv. tomato DC3000, it should be noted that in *P. aeruginosa*, Pvd is thought to be efficiently recycled from the intercellular space to the extracellular medium after iron release, thereby dramatically reducing its associated synthesis cost (37). This is contrasted with ferric enterobactin, where the iron-bound siderophore must be imported into the cytoplasm prior to iron release (45). In this case, the imported Fe-enterobactin is hydrolyzed or chemically modified, permanently lowering its affinity for Fe(III). Though it is unknown how Ybt is utilized, the *P. syringae* pv. tomato DC3000 Ybt cluster contains two putative inner-membrane ABC subfamily B transporters that are highly similar to *ybtP* and *ybtQ* of *Y. pestis* (Fig. 2). In *Y. pestis*, these ABC transporters have been shown to function in Ybt uptake, suggesting intracellular transport of Ybt (32). Furthermore, the time course experiment shows Pvd (but not Ybt) accumulation in culture supernatant over time at late stationary phase (Fig. 9). This result could be explained by the recycling (and thus accumulation) of Pvd contrasted with Ybt turnover, though other explanations are possible (as discussed below). Nevertheless, if Pvd were efficiently recycled by DC3000 while Ybt was not, under conditions where Pvd alone is sufficient for iron acquisition, a Ybt$^-$ mutant could exhibit enhanced growth, as observed. Similarly, under conditions where Pvd was the more effective siderophore, if Ybt competed with Pvd for iron or otherwise interfered with Pvd function, then a Ybt$^-$ mutant would have enhanced growth. However, we cannot exclude Ybt (and/or) SA production negatively affecting fitness independently of iron acquisition under these conditions.

The possibility that Ybt (and/or SA) produced by *P. syringae* pv. tomato DC3000 plays a role other than functioning directly in iron acquisition is intriguing, particularly in the context of plant infection. For example, SA has the ability to alter gene expression in both bacteria and plants. In plants, it acts as a phytohormone responsible for the transcriptional induction of myriad defense-related genes, resulting in systemic acquired resistance (24). In bacteria, SA can impact bacterial virulence through the induction of intrinsic multiple antibiotic resistance (2, 63), enhanced mutation rates, and/or reduced motility (61). In addition, bacterial production of SA by root-associated bacteria may facilitate induced systemic resistance responses in plants (5, 16, 23). Therefore, we were interested in determining whether SA produced by DC3000 in the leaf apoplast could induce defensive responses in the infected leaf. In the *ics1* SA biosynthetic mutant, DC3000 growth is enhanced ~10- to 30-fold at 3 dpi compared with growth in wild-type *Arabidopsis* plants (54). If SA produced by DC3000 partially rescues the SA-deficient *Arabidopsis* phenotype, we might expect to see even greater bacterial growth of the *pchA* mutant compared with DC3000 on the *ics1* mutant plants. We observed no sig-

nificant difference in bacterial growth for the *pchA* versus wild-type DC3000 strains on the *ics1* mutant (Fig. 10C). This result was consistent with our expectations based on the very low level of excreted SA produced by DC3000 in culture. Interestingly, we detected about 10-fold-less excreted SA in supernatants of *P. syringae* pv. tomato DC3000 than in *P. aeruginosa* PAO1 on a cell-normalized basis (data not shown), possibly suggesting a selective pressure on this plant pathogen to limit excreted SA.

Regulation of siderophore production and utilization in *P. syringae* pv. tomato DC3000. In addition to the potential for SA to act as a signaling molecule, high-affinity siderophores themselves can act as signaling molecules. For example, Pvd induces expression of its own biosynthetic genes as well as other virulence factors, including exotoxin A and endoprotease in *P. aeruginosa* (74). This Pvd signaling function is mediated by an additional N-terminal domain of the TonB-dependent Pvd receptor (e.g., FpvA of *P. aeruginosa* PAO1) (43, 66). To determine whether Ybt might act as a signaling molecule using a mechanism similar to that for Pvd, we examined the expression of the Ybt biosynthetic gene *ybtE* in the Ybt$^-$ *pchA* mutant. If Ybt production is required for full induction of expression of the Ybt biosynthetic cluster, we would expect to see little or significantly reduced expression of *ybtE* in the *pchA* mutant. However, we found similarly induced expression of *ybtE* in wild-type and *pchA* mutant strains under iron-limiting conditions (Fig. 10B), suggesting that Ybt gene expression is not regulated by Ybt-dependent signaling. Furthermore, the putative *P. syringae* pv. tomato DC3000 TonB-dependent Ybt receptor FyuA (PSPTO2605), located in the Ybt cluster, does not contain the N-terminal extension required for siderophore-dependent signaling (see Fig. S1 in the supplemental material); thus, amplification of *ybt* gene expression is unlikely to occur via this mechanism. In contrast, there is the potential for Pvd-dependent signaling via a TonB-dependent Pvd receptor in DC3000 as one (FpvA-1; PSPTO2151) of the two adjacent putative *P. syringae* pv. tomato DC3000 Pvd receptors does contain this additional N-terminal domain.

AraC transcriptional regulators can also mediate siderophore-dependent amplification of siderophore biosynthesis (52). In the case of pyochelin production in *P. aeruginosa*, the AraC transcriptional regulator (PchR) directly interacts with ferric pyochelin and thereby mediates ferric pyochelin amplification of pyochelin biosynthesis (52). Perhaps the AraC transcriptional regulator (PSPTO2606) adjacent to the Ybt cluster in DC3000 mediates positive amplification of Ybt biosynthesis by ferric Ybt. However, as stated above, we found wild-type induction of *ybtE* expression in the absence of Ybt formation, suggesting that this is not the case.

In contrast to the atypical lack of siderophore-dependent amplification of expression of siderophore biosynthetic genes observed for Ybt, we observed canonical repression of both Ybt and Pvd biosynthetic gene expression in the presence of high iron levels (50 μM $FeCl_3$). This repression is likely mediated by the ferric uptake regulator FUR (56).

Though we typically observed similar patterns of Pvd and Ybt production under the conditions we assessed in culture, in stationary-phase culture supernatants grown under low-iron conditions, we observed enhanced Pvd compared with declining Ybt (Fig. 9). This could be explained by a cell density-dependent regulation of Pvd versus Ybt biosynthesis, as quorum-sensing *P. aeruginosa* mutants exhibit reduced Pvd production (69). Alternatively, accumulation of a particular product in stationary-phase cultures could differentially impact Pvd versus Ybt metabolism, perhaps by inhibiting Ybt synthesis. Another possibility is that recycling of Pvd (but not Ybt) to the extracellular medium could result in increasing Pvd levels in the culture supernatants over time (as discussed earlier).

Clearly, there is much to learn about the function and regulation of siderophores and their precursors in plant host-bacterial interactions. Here, we provide initial insights, tools, and directions to elucidate the function of SA and siderophore biosynthesis in the important and widely studied phytopathogen *Pseudomonas syringae* pv. *tomato* strain DC3000. The numerous genetic and genomic resources available for both DC3000 and the plant host *Arabidopsis thaliana* make this an extremely attractive pathosystem for elucidating the complex role of iron, SA, and siderophores in plant-pathogen interactions. In addition, the chemical cross-talk that is arguably more readily resolved in plant pathosystems (as numerous plants may be easily generated and assayed) may provide fundamental insights applicable to other host-microbe interactions. For example, *Arabidopsis* is capable of taking up the bacterial siderophore Fe^{3+}-Pvd and utilizing it to rescue iron deficiency (73). As this implies recognition of the bacterial siderophore, it is also possible that plant recognition of specific bacterial siderophores could trigger plant immune responses. The phytopathogen could then respond by modifying the siderophore to evade host recognition or use it as a "Trojan horse" to deliver a toxin, as has been described for other systems (33). It is not known whether Ybt-Fe^{3+} can also be recognized and utilized by plants. However, it is clear that the ability of a given phytopathogen to produce multiple high-affinity siderophores is of great utility, as different siderophores have distinct affinities for iron (and other transition metals [75]), differential pH-dependent stability and affinity, and different associated costs and modes of regulation, and they may be under selective counter-evolutionary pressures with given hosts. We are excited by the prospect of resolving the impact of these features on the evolving functional roles of bacterial siderophores in a tractable plant pathosystem.

ACKNOWLEDGMENTS

We thank Chaitan Khosla (Stanford University) for the Ybt standard and Allis Chien and Lindsay Comeaux of the Vincent Coates Foundation Mass Spectrometry Laboratory (Stanford University) for MS analyses.

This work was supported by University of California—Berkeley StartUp funds provided to M.C.W.

REFERENCES

1. **Abergel, R. J., M. K. Wilson, J. E. Arceneaux, T. M. Hoette, R. K. Strong, B. R. Byers, and K. N. Raymond.** 2006. Anthrax pathogen evades the mammalian immune system through stealth siderophore production. Proc. Natl. Acad. Sci. USA **103:**18499–18503.
2. **Alekshun, M. N., and S. B. Levy.** 1999. The mar regulon: multiple resistance to antibiotics and other toxic chemicals. Trends Microbiol. **7:**410–413.
3. **Alonso, J. M., and J. R. Ecker.** 2006. Moving forward in reverse: genetic technologies to enable genome-wide phenomic screens in Arabidopsis. Nat. Rev. Genet. **7:**524–536.
4. **Anisimov, R., D. Brem, J. Heesemann, and A. Rakin.** 2005. Molecular mechanism of YbtA-mediated transcriptional regulation of divergent overlapping promoters ybtA and irp6 of Yersinia enterocolitica. FEMS Microbiol. Lett. **250:**27–32.

5. **Audenaert, K., T. Pattery, P. Cornelis, and M. Hofte.** 2002. Induction of systemic resistance to Botrytis cinerea in tomato by Pseudomonas aeruginosa 7NSK2: role of salicylic acid, pyochelin, and pyocyanin. Mol. Plant-Microbe Interact. **15:**1147–1156.
6. **Bearden, S. W., J. D. Fetherston, and R. D. Perry.** 1997. Genetic organization of the yersiniabactin biosynthetic region and construction of avirulent mutants in *Yersinia pestis*. Infect. Immun. **65:**1659–1668.
7. **Beattie, G. A., and S. E. Lindow.** 1994. Epiphytic fitness of phytopathogenic bacteria: physiological adaptations for growth and survival. Curr. Top. Microbiol. Immunol. **192:**1–27.
8. **Braun, V.** 2003. Iron uptake by Escherichia coli. Front. Biosci. **8:**S1409–S1421.
9. **Brown, J. C.** 1978. Mechanism of iron uptake by plants. Plant Cell Environ. **1:**249–257.
10. **Buchanan, B. B., and Y. Balmer.** 2005. Redox regulation: a broadening horizon. Annu. Rev. Plant Biol. **56:**187–220.
11. **Buell, C. R., V. Joardar, M. Lindeberg, J. Selengut, I. T. Paulsen, M. L. Gwinn, R. J. Dodson, R. T. Deboy, A. S. Durkin, J. F. Kolonay, R. Madupu, S. Daugherty, L. Brinkac, M. J. Beanan, D. H. Haft, W. C. Nelson, T. Davidsen, N. Zafar, L. Zhou, J. Liu, Q. Yuan, H. Khouri, N. Fedorova, B. Tran, D. Russell, K. Berry, T. Utterback, S. E. Van Aken, T. V. Feldblyum, M. D'Ascenzo, W. L. Deng, A. R. Ramos, J. R. Alfano, S. Cartinhour, A. K. Chatterjee, T. P. Delaney, S. G. Lazarowitz, G. B. Martin, D. J. Schneider, X. Tang, C. L. Bender, O. White, C. M. Fraser, and A. Collmer.** 2003. The complete genome sequence of the *Arabidopsis* and tomato pathogen *Pseudomonas syringae* pv. *tomato* DC3000. Proc. Natl. Acad. Sci. USA **100:**10181–10186.
12. **Bultreys, A., I. Gheysen, and E. de Hoffmann.** 2006. Yersiniabactin production by *Pseudomonas syringae* and *Escherichia coli*, and description of a second yersiniabactin locus evolutionary group. Appl. Environ Microbiol. **72:**3814–3825.
13. **Bultreys, A., I. Gheysen, H. Maraite, and E. de Hoffmann.** 2001. Characterization of fluorescent and nonfluorescent peptide siderophores produced by *Pseudomonas syringae* strains and their potential use in strain identification. Appl. Environ Microbiol. **67:**1718–1727.
14. **Bultreys, A., I. Gheysen, B. Wathelet, H. Maraite, and E. de Hoffmann.** 2003. High-performance liquid chromatography analyses of pyoverdin siderophores differentiate among phytopathogenic fluorescent *Pseudomonas* species. Appl. Environ. Microbiol. **69:**1143–1153.
15. **Bultreys, A., I. Gheysen, B. Wathelet, M. Schafer, and H. Budzikiewicz.** 2004. The pyoverdins of Pseudomonas syringae and Pseudomonas cichorii. Z. Naturforsch. C **59:**613–618.
16. **Buysens, S., K. Heungens, J. Poppe, and M. Hofte.** 1996. Involvement of pyochelin and pyoverdin in suppression of pythium-induced damping-off of tomato by *Pseudomonas aeruginosa* 7NSK2. Appl. Environ. Microbiol. **62:**865–871.
17. **Cendrowski, S., W. MacArthur, and P. Hanna.** 2004. Bacillus anthracis requires siderophore biosynthesis for growth in macrophages and mouse virulence. Mol. Microbiol. **51:**407–417.
18. **Cody, Y. S., and D. C. Gross.** 1987. Characterization of pyoverdin$_{pss}$, the fluorescent siderophore produced by *Pseudomonas syringae* pv. *syringae*. Appl. Environ. Microbiol. **53:**928–934.
19. **Cody, Y. S., and D. C. Gross.** 1987. Outer membrane protein mediating iron uptake via pyoverdin$_{pss}$, the fluorescent siderophore produced by *Pseudomonas syringae* pv. *syringae*. J. Bacteriol. **169:**2207–2214.
20. **Coulthurst, S. J., A. M. Barnard, and G. P. Salmond.** 2005. Regulation and biosynthesis of carbapenem antibiotics in bacteria. Nat. Rev. Microbiol. **3:**295–306.
21. **Crosa, J. H., and C. T. Walsh.** 2002. Genetics and assembly line enzymology of siderophore biosynthesis in bacteria. Microbiol. Mol. Biol. Rev. **66:**223–249.
22. **Cuppels, D. A.** 1986. Generation and characterization of Tn*5* insertion mutations in *Pseudomonas syringae* pv. *tomato*. Appl. Environ. Microbiol. **51:**323–327.
23. **De Meyer, G., K. Capieau, K. Audenaert, A. Buchala, J. P. Metraux, and M. Hofte.** 1999. Nanogram amounts of salicylic acid produced by the rhizobacterium Pseudomonas aeruginosa 7NSK2 activate the systemic acquired resistance pathway in bean. Mol. Plant-Microbe Interact. **12:**450–458.
24. **Dempsey, D. M. A., J. Shah, and D. F. Klessig.** 1999. Salicylic acid and disease resistance in plants. Crit. Rev. Plant Sci. **18:**547–575.
25. **Dewdney, J., T. L. Reuber, M. C. Wildermuth, A. Devoto, J. Cui, L. M. Stutius, E. P. Drummond, and F. M. Ausubel.** 2000. Three unique mutants of *Arabidopsis* identify *eds* loci required for limiting growth of a biotrophic fungal pathogen. Plant J. **24:**205–218.
26. **Drechsel, H., H. Stephan, R. Lotz, H. Haag, H. Zahner, K. Hantke, and G. Jung.** 1995. Structural elucidation of yersiniabactin, a siderophore from highly virulent Yersinia strains. Leibigs Ann. **10:**1727–1733.
27. Reference deleted.
28. **Eichhorn, H., F. Lessing, B. Winterberg, J. Schirawski, J. Kamper, P. Muller, and R. Kahmann.** 2006. A ferroxidation/permeation iron uptake system is required for virulence in Ustilago maydis. Plant Cell **18:**3332–3345.
29. **Enard, C., A. Diolez, and D. Expert.** 1988. Systemic virulence of *Erwinia chrysanthemi* 3937 requires a functional iron assimilation system. J. Bacteriol. **170:**2419–2426.
30. **Expert, D.** 1999. Withholding and exchanging iron: interactions between Erwinia spp. and their plant hosts. Annu. Rev. Phytopathol. **37:**307–334.
31. **Felle, H. H.** 2006. Apoplastic pH during low-oxygen stress in barley. Ann. Bot. (London) **98:**1085–1093.
32. **Fetherston, J. D., V. J. Bertolino, and R. D. Perry.** 1999. YbtP and YbtQ: two ABC transporters required for iron uptake in Yersinia pestis. Mol. Microbiol. **32:**289–299.
33. **Fischbach, M. A., H. Lin, D. R. Liu, and C. T. Walsh.** 2006. How pathogenic bacteria evade mammalian sabotage in the battle for iron. Nat. Chem. Biol. **2:**132–138.
34. **Franza, T., B. Mahe, and D. Expert.** 2005. Erwinia chrysanthemi requires a second iron transport route dependent on the siderophore achromobactin for extracellular growth and plant infection. Mol. Microbiol. **55:**261–275.
35. **Gao, D., M. R. Knight, A. J. Trewavas, B. Sattelmacher, and C. Plieth.** 2004. Self-reporting Arabidopsis expressing pH and [Ca^{2+}] indicators unveil ion dynamics in the cytoplasm and in the apoplast under abiotic stress. Plant Physiol. **134:**898–908.
36. **Glazebrook, J., E. E. Rogers, and F. M. Ausubel.** 1996. Isolation of Arabidopsis mutants with enhanced disease susceptibility by direct screening. Genetics **143:**973–982.
37. **Greenwald, J., F. Hoegy, M. Nader, L. Journet, G. L. Mislin, P. L. Graumann, and I. J. Schalk.** 2007. Real time fluorescent resonance energy transfer visualization of ferric pyoverdine uptake in Pseudomonas aeruginosa. A role for ferrous iron. J. Biol. Chem. **282:**2987–2995.
38. **Griffiths, E.** 1978. Iron in biological systems. *In* J. J. Bullen and E. Griffiths (ed.), Iron and infection. John Wiley and Sons, Hoboken, NJ.
39. **Guerinot, M. L.** 1994. Microbial iron transport. Annu. Rev. Microbiol. **48:**743–772.
40. **Haag, H., K. Hantke, H. Drechsel, I. Stojiljkovic, G. Jung, and H. Zahner.** 1993. Purification of yersiniabactin: a siderophore and possible virulence factor of Yersinia enterocolitica. J. Gen. Microbiol. **139:**2159–2165.
41. **Hirano, S. S., and C. D. Upper.** 2000. Bacteria in the leaf ecosystem with emphasis on *Pseudomonas syringae*—a pathogen, ice nucleus, and epiphyte. Microbiol. Mol. Biol Rev. **64:**624–653.
42. **Huang, W. E., L. Huang, G. M. Preston, M. Naylor, J. P. Carr, Y. Li, A. C. Singer, A. S. Whiteley, and H. Wang.** 2006. Quantitative in situ assay of salicylic acid in tobacco leaves using a genetically modified biosensor strain of Acinetobacter sp. ADP1. Plant J. **46:**1073–1083.
43. **James, H. E., P. A. Beare, L. W. Martin, and I. L. Lamont.** 2005. Mutational analysis of a bifunctional ferrisiderophore receptor and signal-transducing protein from *Pseudomonas aeruginosa*. J. Bacteriol. **187:**4514–4520.
44. **Katagiri, F., R. Thilmony, and S. Y. He.** 27 March 2002, posting date. The *Arabidopsis thaliana-Pseudomonas syringae* interaction. *In* C. R. Somerville and E. M. Meyerowitz (ed.), The *Arabidopsis* book. American Society of Plant Biologists, Rockville, MD. doi:10.1199/tab.0039.
45. **Langman, L., I. G. Young, G. E. Frost, H. Rosenberg, and F. Gibson.** 1972. Enterochelin system of iron transport in *Escherichia coli*: mutations affecting ferric-enterochelin esterase. J. Bacteriol. **112:**1142–1149.
46. **Lawlor, M. S., C. O'Connor, and V. L. Miller.** 2007. Yersiniabactin is a virulence factor for *Klebsiella pneumoniae* during pulmonary infection. Infect. Immun. **75:**1463–1472.
47. **Leong, S. A., and J. B. Neilands.** 1981. Relationship of siderophore-mediated iron assimilation to virulence in crown gall disease. J. Bacteriol. **147:**482–491.
48. **Lopez-Millan, A. F., F. Morales, A. Abadia, and J. Abadia.** 2000. Effects of iron deficiency on the composition of the leaf apoplastic fluid and xylem sap in sugar beet. Implications for iron and carbon transport. Plant Physiol. **124:**873–884.
49. **Lopez-Millan, A. F., F. Morales, A. Abadia, and J. Abadia.** 2001. Iron deficiency-associated changes in the composition of the leaf apoplastic fluid from field-grown pear (Pyrus communis L.) trees. J. Exp. Bot. **52:**1489–1498.
50. **Melotto, M., W. Underwood, J. Koczan, K. Nomura, and S. Y. He.** 2006. Plant stomata function in innate immunity against bacterial invasion. Cell **126:**969–980.
51. **Meyer, J. M., A. Neely, A. Stintzi, C. Georges, and I. A. Holder.** 1996. Pyoverdin is essential for virulence of *Pseudomonas aeruginosa*. Infect. Immun. **64:**518–523.
52. **Michel, L., N. Gonzalez, S. Jagdeep, T. Nguyen-Ngoc, and C. Reimmann.** 2005. PchR-box recognition by the AraC-type regulator PchR of Pseudomonas aeruginosa requires the siderophore pyochelin as an effector. Mol. Microbiol. **58:**495–509.
53. **Mossialos, D., U. Ochsner, C. Baysse, P. Chablain, J. P. Pirnay, N. Koedam, H. Budzikiewicz, D. U. Fernandez, M. Schafer, J. Ravel, and P. Cornelis.** 2002. Identification of new, conserved, non-ribosomal peptide synthetases from fluorescent pseudomonads involved in the biosynthesis of the siderophore pyoverdine. Mol. Microbiol. **45:**1673–1685.
54. **Nawrath, C., and J. P. Metraux.** 1999. Salicylic acid induction-deficient mutants of Arabidopsis express PR-2 and PR-5 and accumulate high levels of camalexin after pathogen inoculation. Plant Cell **11:**1393–1404.
55. **Neidhardt, F. C., P. L. Bloch, and D. F. Smith.** 1974. Culture medium for enterobacteria. J. Bacteriol. **119:**736–747.

56. **Ochsner, U. A., A. I. Vasil, and M. L. Vasil.** 1995. Role of the ferric uptake regulator of *Pseudomonas aeruginosa* in the regulation of siderophores and exotoxin A expression: purification and activity on iron-regulated promoters. J. Bacteriol. **177:**7194–7201.
57. **Oide, S., W. Moeder, S. Krasnoff, D. Gibson, H. Haas, K. Yoshioka, and B. G. Turgeon.** 2006. NPS6, encoding a nonribosomal peptide synthetase involved in siderophore-mediated iron metabolism, is a conserved virulence determinant of plant pathogenic ascomycetes. Plant Cell **18:**2836–2853.
58. **Perry, R. D., P. B. Balbo, H. A. Jones, J. D. Fetherston, and E. DeMoll.** 1999. Yersiniabactin from Yersinia pestis: biochemical characterization of the siderophore and its role in iron transport and regulation. Microbiology **145:**1181–1190.
59. **Pfeifer, B. A., C. C. Wang, C. T. Walsh, and C. Khosla.** 2003. Biosynthesis of yersiniabactin, a complex polyketide-nonribosomal peptide, using *Escherichia coli* as a heterologous host. Appl. Environ Microbiol. **69:**6698–6702.
60. **Poole, K., and G. A. McKay.** 2003. Iron acquisition and its control in Pseudomonas aeruginosa: many roads lead to Rome. Front. Biosci. **8:**661–686.
61. **Price, C. T., I. R. Lee, and J. E. Gustafson.** 2000. The effects of salicylate on bacteria. Int. J. Biochem. Cell Biol. **32:**1029–1043.
62. **Ratledge, C., and L. G. Dover.** 2000. Iron metabolism in pathogenic bacteria. Annu. Rev. Microbiol. **54:**881–941.
63. **Ravirala, R. S., R. D. Barabote, D. M. Wheeler, S. Reverchon, O. Tatum, J. Malouf, H. Liu, L. Pritchard, P. E. Hedley, P. R. Birch, I. K. Toth, P. Payton, and M. J. San Francisco.** 2007. Efflux pump gene expression in Erwinia chrysanthemi is induced by exposure to phenolic acids. Mol. Plant-Microbe Interact. **20:**313–320.
64. **Reimmann, C., L. Serino, M. Beyeler, and D. Haas.** 1998. Dihydroaeruginoic acid synthetase and pyochelin synthetase, products of the pchEF genes, are induced by extracellular pyochelin in Pseudomonas aeruginosa. Microbiology **144:**3135–3148.
65. **Rondon, M. R., K. S. Ballering, and M. G. Thomas.** 2004. Identification and analysis of a siderophore biosynthetic gene cluster from Agrobacterium tumefaciens C58. Microbiology **150:**3857–3866.
66. **Schalk, I. J., W. W. Yue, and S. K. Buchanan.** 2004. Recognition of iron-free siderophores by TonB-dependent iron transporters. Mol. Microbiol. **54:**14–22.
67. **Serino, L., C. Reimmann, H. Baur, M. Beyeler, P. Visca, and D. Haas.** 1995. Structural genes for salicylate biosynthesis from chorismate in Pseudomonas aeruginosa. Mol. Gen. Genet. **249:**217–228.
68. **Serino, L., C. Reimmann, P. Visca, M. Beyeler, V. D. Chiesa, and D. Haas.** 1997. Biosynthesis of pyochelin and dihydroaeruginoic acid requires the iron-regulated *pchDCBA* operon in *Pseudomonas aeruginosa*. J. Bacteriol. **179:**248–257.
69. **Stintzi, A., K. Evans, J. M. Meyer, and K. Poole.** 1998. Quorum-sensing and siderophore biosynthesis in Pseudomonas aeruginosa: lasR/lasI mutants exhibit reduced pyoverdine biosynthesis. FEMS Microbiol. Lett. **166:**341–345.
70. **Strawn, M. A., S. K. Marr, K. Inoue, N. Inada, C. Zubieta, and M. C. Wildermuth.** 2007. Arabidopsis isochorismate synthase functional in pathogen-induced salicylate biosynthesis exhibits properties consistent with a role in diverse stress responses. J. Biol. Chem. **282:**5919–5933.
71. **Tindale, A. E., M. Mehrotra, D. Ottem, and W. J. Page.** 2000. Dual regulation of catecholate siderophore biosynthesis in Azotobacter vinelandii by iron and oxidative stress. Microbiology **146:**1617–1626.
72. **Valdebenito, M., A. L. Crumbliss, G. Winkelmann, and K. Hantke.** 2006. Environmental factors influence the production of enterobactin, salmochelin, aerobactin, and yersiniabactin in Escherichia coli strain Nissle 1917. Int J. Med. Microbiol. **296:**513–520.
73. **Vansuyt, G., A. Robin, J. F. Briat, C. Curie, and P. Lemanceau.** 2007. Iron acquisition from Fe-pyoverdine by Arabidopsis thaliana. Mol. Plant-Microbe Interact. **20:**441–447.
74. **Vasil, M. L.** 2007. How we learnt about iron acquisition in Pseudomonas aeruginosa: a series of very fortunate events. Biometals **20:**587–601.
75. **Visca, P., G. Colotti, L. Serino, D. Verzili, N. Orsi, and E. Chiancone.** 1992. Metal regulation of siderophore synthesis in *Pseudomonas aeruginosa* and functional effects of siderophore-metal complexes. Appl. Environ. Microbiol. **58:**2886–2893.
76. **Visca, P., L. Leoni, M. J. Wilson, and I. L. Lamont.** 2002. Iron transport and regulation, cell signalling and genomics: lessons from Escherichia coli and Pseudomonas. Mol. Microbiol. **45:**1177–1190.
77. **Whalen, M. C., R. W. Innes, A. F. Bent, and B. J. Staskawicz.** 1991. Identification of *Pseudomonas syringae* pathogens of *Arabidopsis* and a bacterial locus determining avirulence on both *Arabidopsis* and soybean. Plant Cell **3:**49–59.
78. **Wienk, K. J., J. J. Marx, and A. C. Beynen.** 1999. The concept of iron bioavailability and its assessment. Eur. J. Nutr. **38:**51–75.
79. **Wildermuth, M. C., J. Dewdney, G. Wu, and F. M. Ausubel.** 2001. Isochorismate synthase is required to synthesize salicylic acid for plant defence. Nature **414:**562–565.